BIOCHEMISTRY
including biophysical chemistry & molecular biology
Article

Biochemistry **2010,** *49,* 7665–7673 7665
DOI: 10.1021/bi100878q

Molecular Simulations of Lipid Flip-Flop in the Presence of Model Transmembrane Helices[†]

Nicolas Sapay,[‡] W. F. Drew Bennett, and D. Peter Tieleman*

Department of Biological Sciences, University of Calgary, 2500 University Drive, Calgary, Alberta T2N 1N4, Canada
[‡]Present address: CERMAV, UPR5301 CNRS, Institut de Chimie Moléculaire de Grenoble, Université de Grenoble, 601 rue de la chimie, BP 53, 38041 Grenoble, France

Received June 2, 2010; Revised Manuscript Received July 22, 2010

ABSTRACT: The transport of lipids between membrane leaflets, also known as flip-flop, is a key process in regulating the lipid composition of biological membranes. It is also important for the growth of biogenic membranes that are the site for lipid synthesis. It has been shown that the mere presence of transmembrane α-helical peptides or proteins enhances the rate lipid flip-flop [Kol et al. (2001) *Biochemistry 40*, 10500−10506]. Using computational models of natural phospholipids with different headgroups, we calculated the free energy profiles for transferring single phospholipids from bulk water to the center of a dioleylphosphatidylcholine (DOPC) bilayer in the presence of transmembrane helices. The free energy barrier for phosphatidylethanolamine (PE) and phosphatidylglycerol (PG) flip-flop decreased by a few kilojoules per mole when a WALP23 or KALP23 peptide was present in the membrane, while the barrier for PC was not affected. We observed large bilayer deformations during lipid flip-flop when the hydrophilic headgroup is in the hydrophobic interior of the bilayer. The presence of KALP23 or WALP23 decreased the size and stability of these defects, suggesting integral membrane proteins affect the mechanism of flip-flop. There was a large decrease in the free energy of desorption for PE and PG when transmembrane peptides were present. This suggests specific PE and PG interactions with the peptide have a large affect on their stability in the membrane, with implications on cellular lipid and protein trafficking.

Lipid bilayers are the core structure of biological membranes. The lipid composition of each of the two membrane leaflets depends on the cell type and compartment and is not necessarily symmetric. In general, the cytoplasmic leaflet of an eukaryotic plasma membrane is enriched in phosphatidylethanolamine (PE)[1] and phosphatidylserine (PS) while the external leaflet is enriched in phosphatidylcholine (PC) and sphingomyelin (*1*, *2*). Breaking this asymmetrical composition by the exposure of PS to the outer leaflet has been linked to a variety of signaling events such as blood coagulation and apoptosis (*3*−*5*). In the endoplasmic reticulum (ER), the bilayer composition is approximately symmetrical (*6*, *7*), although the cytosolic leaflet has phospholipid synthase activity. A rapid translocation of phospholipids is required to allow a uniform growth of its inner and outer leaflets (*8*).

Lipid translocation, or flip-flop, occurs spontaneously in pure lipid bilayers at a very slow rate with half-times on the order of hours (*9*). In contrast, half-times measured in living cells or reconstituted membranes range from seconds to minutes (*7*, *10*, *11*) and suggest that general lipid translocation is protein mediated. While specific amino-phospholipid flippases have been identified, the characterization of specific lipid translocators remains elusive.

Specifically, a general lipid translocator in the ER membrane, necessary for the rapid flip-flop and symmetric lipid distribution, has not been identified. This flip-flop activity has been shown to be protein-mediated, bidirectional, ATP-independent, and not specific for the phospholipid headgroup (*12*). De Kruijff and colleagues have shown that flip-flop of lipid analogues is enhanced by the mere presence of helical transmembrane segments (*12*−*14*). Typically, the flip-flop rate of a phosphatidylglycerol (PG) analogue increases from 0.03 to 0.17 h^{-1} in the presence of the WALP23 transmembrane peptide (*14*). Similar observations have been made with the KALP23 peptide (*12*) or transmembrane helical proteins (*14*) but not with transmembrane β-barrel proteins (*14*). Noteworthy, the effect of transmembrane peptides depends on their concentration (*13*) and does not show saturation in the range of concentrations tested (1:250 to 1:2000 peptide:lipid ratios). This effect also depends on the lipid headgroup. A large enhancement of the rate of flip-flop has been observed for PG analogues but not for PC analogues (*12*). Flip-flop in the presence of transmembrane peptides also depends on the lipid composition. For example, addition of PE or cholesterol in PC vesicles decreases the flip-flop rate (*12*).

In cells, there is a large difference in membrane composition and structure, but how lipids and membrane proteins are trafficked and sorted is not fully understood (*2*). The difference in free energy between a lipid at equilibrium in a bilayer and bulk

[†]This work is supported by Canadian Institutes of Health Research (CIHR). W.F.D.B. is supported by studentships from the National Science and Engineering Research Council (NSERC), Alberta Heritage Foundation for Medical Research (AHFMR), and the Killam Trust. D.P.T. is an Alberta Heritage Foundation for Medical Research Scientist.

*Corresponding author: e-mail, tieleman@ucalgary.ca; phone, 403-220-2966; fax, 403-289-9311.

[1]Abbreviations: DOPC, dioleoylphosphatidylcholine; DOPE, dioleoylphosphatidylethanolamine, DOPG, dioleoylphosphatidylglycerol; MD, molecular dynamics; PMF, potential of mean force; ER, endoplasmic reticulum.

Published on Web 07/28/2010

Table 1: Summary of the Simulated Bilayers[a]

system	bilayer	restrained lipid	peptide	$N_{simulation}$	time/simulation
DOPC	62 DOPC	2 DOPC		45	60
DOPC + WALP23	62 DOPC	2 DOPC	WALP23	45	50
DOPC + KALP23	62 DOPC	2 DOPC	KALP23	45	70
DOPE	62 DOPC	2 DOPE		45	60
DOPE + WALP23	62 DOPC	2 DOPE	WALP23	45	90
DOPE + KALP23	62 DOPC	2 DOPE	KALP23	45	90
DOPG	62 DOPC	2 DOPG		45	120
DOPG + WALP23	62 DOPC	2 DOPG	WALP23	45	90
DOPG + KALP23	62 DOPC	2 DOPG	KALP23	45	120

[a]Bilayers were symmetric with 31 DOPC lipids per leaflet and one restrained lipid. $N_{simulation}$ is the number of independent simulations performed per system. Times are in nanoseconds.

water is the free energy for desorption and can be equated to the excess chemical potential of the lipid in a bilayer compared to water. Comparing a lipid's excess chemical potential in two different membrane environments allows one to infer its preferred location. We can determine the thermodynamic basis for a lipid's stability in a particular membrane environment at atomistic resolution. The excess chemical potential for DPPC in a DPPC bilayer compared to water was calculated and compared well to the free energy expected from the experimental critical micelle concentration of DPPC (*15*).

Molecular dynamics (MD) simulations provide atomistic resolution thermodynamic data on model membrane systems. Previously, MD simulations showed that DPPC flip-flop occurs through a pore-mediated mechanism, and the rate of flip-flop was determined to be hours to days (*15*), in agreement with experimental estimates. By inducing pore formation using an ionic charge imbalance, Gurtovenko and Vattulainen showed that DMPC could diffuse across the pore on the time scale of tens of nanoseconds (*16*). Similar results were obtained when dimethylsulfoxide was added to a bilayer system; transient pores were induced, and PC flip-flop was observed within tens of nanoseconds (*17*). The major energetic barrier for flip-flop is the formation of transient water defects and pores. We showed that increasing the concentration of cholesterol in DPPC bilayers prevented pore formation and decreased the rate of flip-flop by orders of magnitude (*18*). Studying the effect of acyl-tail length and degree of unsaturation showed that flip-flop is much faster in PC lipids with shorter tails (*19*). The use of computer simulations to study flip-flop and membrane pores and defects has been recently reviewed (*20*).

In the present work, we have investigated lipid flip-flop in the presence of WALP23 and KALP23 using molecular dynamics. We have calculated the free energy for transferring DOPC, DOPE, or DOPG from bulk water to the center of a pure DOPC bilayer or in the presence of WALP23 or KALP23. Those calculations give an estimate of the free energy barrier for flip-flop and lipid desorption.

METHODS

System Setup and Molecular Simulations. The partitioning of DOPC, DOPE, or DOPG was studied in three systems summarized in Table 1. The OPLS-AA force field was used for the peptides and the ions (*21*). Water was modeled with the simple point charge model (*22*). This combination has been tested previously and found to yield relatively accurate water−cyclohexane transfer free energies (*23*). The initial coordinates were taken from preequilibrated systems used in previous studies (*23*). Lipid parameters were a development version and are available on request.

All simulations were carried out with GROMACS 3.3.1 (*24*). We used a time step of 2 fs and Lennard-Jones potential cutoff at 0.9 nm, and electrostatic interactions were treated using the particle mesh Ewald method (*25*, *26*) with a grid spacing of viz. 0.1 nm and a real-space cutoff of 0.9 nm. Sodium or chlorine ions were added when required to neutralize systems. The temperature and the pressure were kept constant at 323 K and 1 bar, respectively, using a Berendsen coupling scheme (*27*) with a compressibility of 4.5×10^{-5} bar^{-1} and a coupling constant of 0.1 ps for temperature and 2.5 ps for pressure. The pressure coupling was semiisotropic. All protein and lipid bonds were constrained with the LINCS algorithm (*28*). Water bonds and angles were constrained with the SETTLE algorithm (*29*).

Umbrella sampling was used to calculate free energy profiles for partitioning of DOPC, DOPE, and DOPG into a DOPC bilayer. A harmonic restraint with a force constant of 3500 kJ mol^{-1} nm^{-2} was applied to the distance between the phosphate of the pulled lipid and the center of mass of the unrestrained lipids forming the bilayer, in the direction normal to the bilayer. There was 0.1 nm spacing between biasing potentials, with a total of 45 simulations for each system. Two phosphates were offset at the same time, so that when the first restrained lipid was at the center of the bilayer and the second one was in bulk water. Carrying out the simulations in this way allows additional statistics to be calculated at essentially no cost. The two phosphates are always at least 4.4 nm apart, i.e., approximately the size of the regular DOPC bilayer. We have shown previously that having two charged molecules spaced at 3.6 nm did not significantly affect its PMF (*30*). Additionally, the PMF for transferring a DPPC molecule from water to the center of a DPPC bilayer was not significantly affected whether one DPPC molecule was restrained or whether two were restrained, separated by 4.2 nm (unpublished data). Before a production run, each window was equilibrated for 1 ns with a force constant of 1000 kJ mol^{-1} nm^{-2} and then 5 ns with a force constant of 3500 kJ mol^{-1} nm^{-2}. Finally, simulations were run for 50−120 ns. The weighted histogram analysis method (*31*) was used to calculate the PMFs from the biased distributions. As two lipids were restrained for each window, the error could be estimated by the difference between the two PMFs. We judged the length of the simulation on the convergence of the PMFs obtained independently from the two leaflets.

Trajectory analysis and visualization were performed with the tools included in the GROMACS package, VMD 1.8.6 (*32*) or

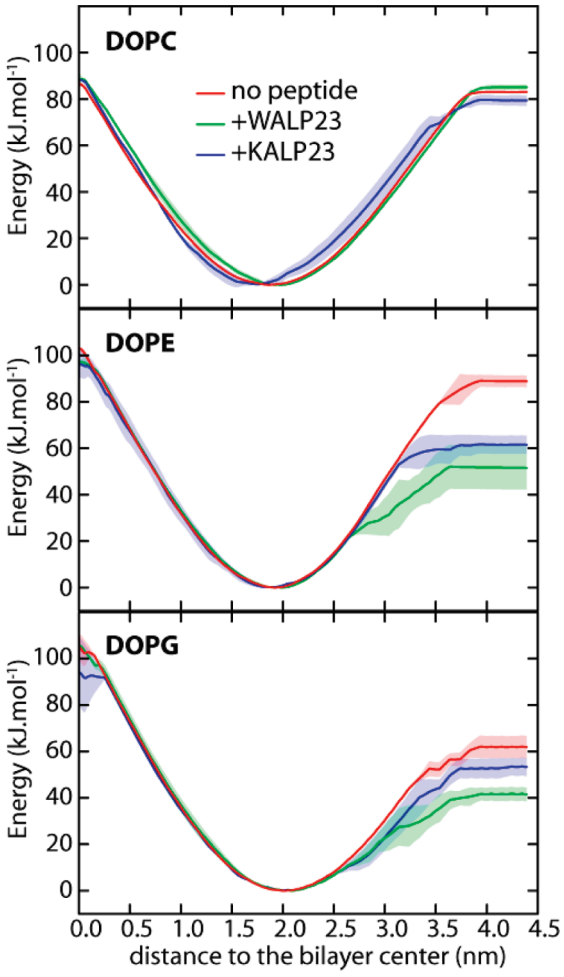

FIGURE 1: Potentials of mean force for DOPC, DOPE, and DOPG in a DOPC bilayer with and without a WALP23 or a KALP23 peptide. Distance is between the center of mass of the bilayer and the phosphate of the restrained lipid. Error bars represent the estimated error from the two independent PMFs. The energy was set to zero at the minimum of the curves, not to suggest the lipid free energy of solvation in a bilayer is the same in all systems. The color code is the same for all panels.

specifically developed tools. Image rendering was done with POV-Ray 3.6.1 (www.povray.org).

RESULTS

Potentials of Mean Force. Figure 1 shows PMFs for transferring a DOPC, DOPE, or DOPG lipid from bulk water to the center of a DOPC bilayer, with and without peptides. The PMFs describe the free energy required for deviations of an individual lipid from its equilibrium position along the transmembrane axis. The well depth in the PMF corresponds to the equilibrium position of the lipid in the bilayer. The position of this minimum is consistent with the phosphate density peak at equilibrium (data not shown), as we restrained the position of the phosphate moiety. There is a steep slope in free energy as the phosphate moves toward the bilayer center, due to the zwitterionic headgroup of PC and PE and the charged headgroup of PG interacting with the hydrophobic interior of the bilayer. A steep slope is observed when the lipid moves into bulk water, as expected from the low solubility of phospholipids in water. A plateau appears when the lipid stops interacting with the bilayer and therefore is the free energy of transferring the lipid to bulk water. It should be noted that the error bars for the PMFs are large, especially in the presence of peptide, reflecting the difficulty of averaging over the motions in a complex membrane system. Error bars are also larger for systems containing DOPG, notably around the center of the bilayer.

Table 2: Free Energy of Flip-Flop ΔG_{flop} and Desorption Free Energy $\Delta G_{desorption}$[a]

system	ΔG_{flop}	δ_{flop}	$d_{z=0}$	$\Delta G_{desorption}$	$\delta_{desorption}$
DOPC	87 ± 1	0		83 ± 0	0
DOPC + WALP23	89 ± 2	2 ± 3	0.43 ± 0.34	85 ± 1	2 ± 1
DOPC + KALP23	88 ± 1	2 ± 2	0.39 ± 0.28	79 ± 2	−4 ± 2
DOPE	103 ± 0	0		89 ± 2	0
DOPE + WALP23	97 ± 1	−6 ± 1	0.39 ± 0.26	52 ± 9	−37 ± 10
DOPE + KALP23	96 ± 6	−7 ± 6	0.38 ± 0.15	61 ± 4	−27 ± 5
DOPG	105 ± 6	0		62 ± 5	0
DOPG + WALP23	106 ± 1	1 ± 6	0.21 ± 0.14	41 ± 3	−17 ± 6
DOPG + KALP23	94 ± 15	−11 ± 16	0.22 ± 0.14	53 ± 4	−6 ± 6

[a] δ_{flop} is the absolute difference between flip-flop free energies with and without peptide, and $\delta_{desorption}$ is the absolute difference between desorption free energies with and without peptide. All energy values are in kJ mol^{-1}. $d_{z=0}$ is the average distance (in nm) in the xy plane (i.e., the plane of the bilayer) between the center of mass of the peptide and the phosphate restrained at the center of the bilayer. The error estimate is shown for each of value.

Lipid Flip-Flop. Table 2 summarizes the free energy barriers for flip-flop, ΔG_{flop}. We assume the primary free energy barrier for flip-flop is the difference in free energy between the center of the bilayer (0 nm) and the lipid's equilibrium position.

In absence of peptide, DOPC has the lowest free energy barrier for flip-flop followed by DOPE and then DOPG. We note that DOPG has a negatively charged headgroup, while both DOPE and DOPC are zwitterionic. Another large difference in headgroup is that the choline of DOPC is not able to form hydrogen bonds, while the ethanolamine and glycerol groups are hydrogen bond donors and PG is also a hydrogen bond acceptor.

ΔG_{flop} for DOPC remains approximately unchanged when either KALP23 or WALP23 is present in the bilayer. For DOPE, ΔG_{flop} decreases by 6 and 7 kJ mol^{-1} when WALP23 and KALP23 are present. The inclusion of WALP23 did not significantly affect ΔG_{flop} for DOPG, but KALP23 resulted in a decrease of 11 kJ mol^{-1}. Although the restraint was applied to the phosphate along the bilayer normal and not in the plane of the bilayer, the lipids remain close to the peptides in all of the simulations (Table 2). The lipid−peptide distance in the bilayer plane is below 0.45 nm, while the length of the simulation box in the plane of the bilayer is approximately 5 nm. Despite the interaction between the lipid and peptide, overall the differences in ΔG_{flop} between systems with and without peptide are relatively small.

Water Defects. When the lipid headgroups are exposed to the hydrophobic interior of the bilayer, a water defect forms to keep the headgroup solvated. Figure 2 shows the water defects that form when a lipid is restrained at the center of the bilayer. For each system, the water density map shows that water is always present around the lipid headgroup and is usually located only on one side of the bilayer (Figure 2, left panels). This bulge of water in the hydrophobic core of the bilayer is accompanied by a deformation of the membrane surface, as shown by the phosphate density maps (Figure 2, right panels). The phosphate density does not reach the center of the bilayer; it drops off on average half way between the normal phosphate density peak and the bilayer center.

For DOPC, the deformation of the membrane surface is almost equally pronounced with and without peptide; a large quantity of water constantly solvates the PC headgroup of the restrained lipid.

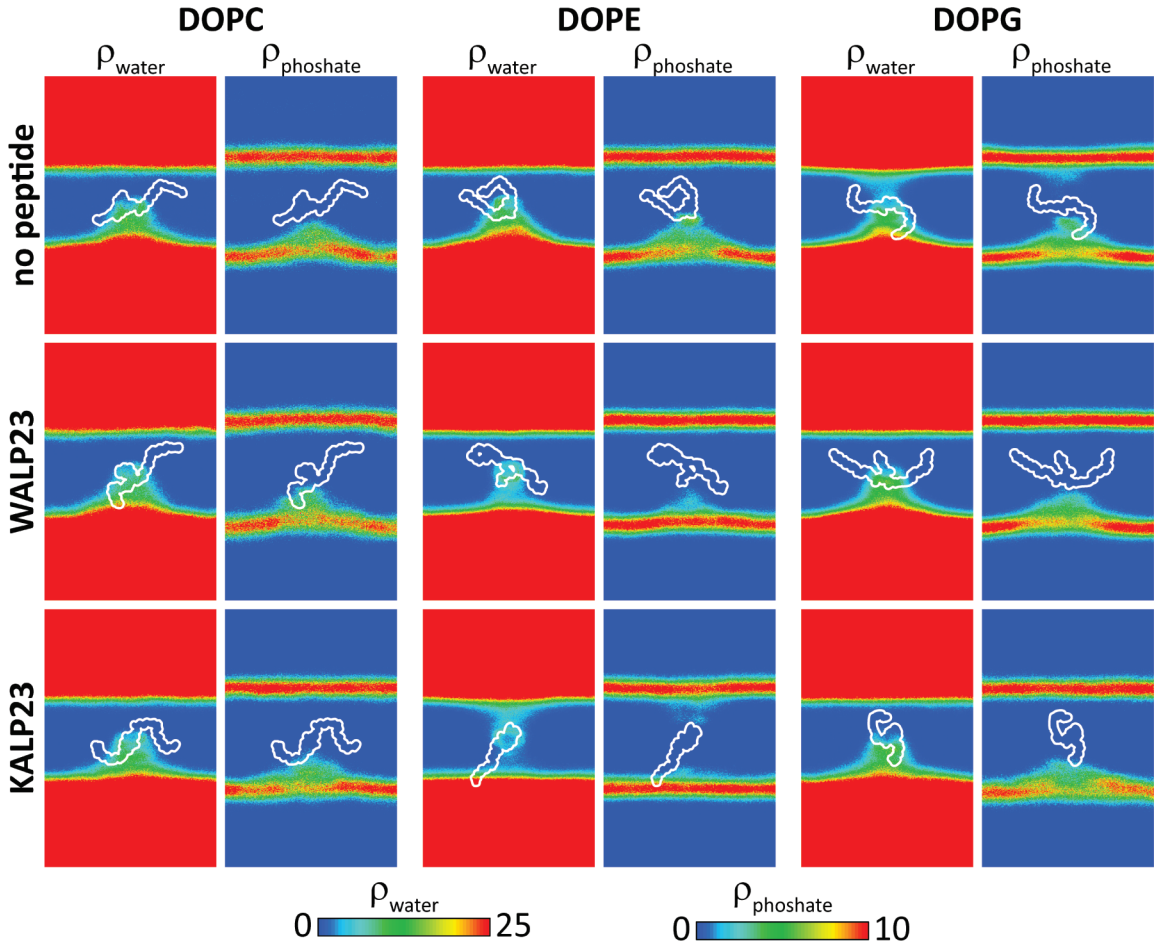

FIGURE 2: Representation of the water defect formed when a DOPC, DOPE, or DOPG lipid is restrained at the center of a DOPC bilayer, with or without peptide. Each panel contains the two-dimensional water and phosphate density maps (left and right, respectively) averaged over the trajectory and the box width. The color scale of the water and phosphate densities are displayed below the panels and correspond to the absolute density in nm^{-3}. For clarity, the scales range from 0 to the maximum density of their respective compound. For each map, the restrained lipid is represented to scale outlined in white. Its conformation is extracted from the last step of the trajectory. All maps are at the same scale.

The presence of peptide visibly reduces the size of the water defect for DOPE, the phosphate density penetrates less deeply into the bilayer core, and the membrane surface is less deformed. Additionally, the water solvating the restrained phosphate does not form a large bulge but rather a thin water link that connects it to the bulk water. This water link occasionally breaks, and the membrane surface becomes flat, similar to a bilayer at equilibrium. We refer to this structure as a broken defect. The water defect then reappears, but not necessarily on the same side. This phenomenon is clearly seen in the KALP23 + DOPE density maps (Figure 2, bottom center), where the water density is high on one side of the restrained lipid and low, but not zero, on the other.

For DOPG, the amount of water within the bilayer is approximately the same as for DOPC, although the phosphate density seems to penetrate less deeply into the bilayer. Occasionally, a double water defect (one per leaflet) appears, only connected via the DOPG headgroup. We do not consider this structure to be a genuine water pore because it is not continuously lined with lipid headgroups and water did not diffuse across it. This configuration occasionally lasts several nanoseconds, after which one of the defects disappears and a regular water defect is formed again. The new water defect was not necessarily on the same side of the bilayer. On several occasions, the water defect flipped from one side to the other within a few picoseconds.

Table 3: Water Defect Characterization[a]

system	double defects	lifetime (ns)	broken defects	lifetime (ns)
DOPC	0		0	
DOPC + WALP23	1	10	3	8
DOPC + KALP23	0		3	25
DOPE	1	6	4	8
DOPE + WALP23	0		4	62
DOPE + KALP23	0		4	34
DOPG	4	15	0	
DOPG + WALP23	0		1	33
DOPG + KALP23	1	7	0	

[a]Number and average lifetime of double and broken water defects observed when the restrained lipid is located within 0.1 nm of the center. The lifetimes are estimated by visualizing the simulations.

Table 3 summarizes the number of double and broken water defects. Their lifetime varies significantly even for the same system, from a few to more than a hundred nanoseconds. Double defects are rare compared to broken defects and mainly observed in systems with DOPG. Broken defects are more abundant and have a longer lifetime in systems with DOPE (up to 180 ns). On average, we observed broken defects more often when a peptide was present in the system. However, the presence of peptide did not affect the hydration of the restrained lipids, as shown by Figure 3.

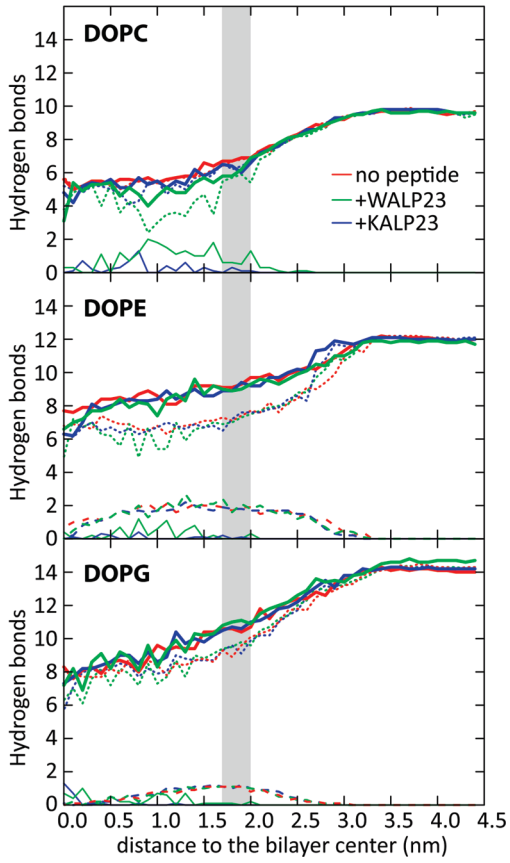

FIGURE 3: Number of hydrogen bonds with the restrained lipid as a function of the distance to the center of the bilayer. Numbers are averaged over the trajectory and the two restrained lipids. The total number of hydrogen bonds is represented by a thick solid line, those with water by a dotted line, those with the bilayer by a dashed line, and those with the peptides by a thin line. The approximate equilibrium position of restrained lipids is represented by a gray shade. The color code is the same for all panels. Note that restrained DOPCs do not form hydrogen bonds with the rest of the bilayer.

There is no marked difference in the number of hydrogen bonds the restrained lipid forms with water in the presence or absence of peptide (Figure 3). We used a simple geometric definition for a hydrogen bond: a distance cutoff of 0.35 nm and angle lower than 30° between the donor and acceptor. In bulk water, DOPE and DOPG form more hydrogen bonds than DOPC because they are capable of being donors and acceptors, while DOPC is not. At the bilayer center DOPC, DOPE, and DOPG form approximately 5, 7, and 8 hydrogen bonds with water. With their donating groups, DOPE and DOPG can form hydrogen bonds with DOPC. Lipid−lipid hydrogen bonds decrease from two (DOPE) and one (DOPG) at equilibrium to zero at the center of the bilayer and are not affected by the presence of peptides. The restrained lipid can form hydrogen bonds with the peptides, especially KALP23 because of the four lysine residues. The number of lipid−peptide hydrogen bonds fluctuates between zero and two, from the equilibrium position and the center of the bilayer. This fluctuation illustrates that sampling may not be complete in the presence of peptide and is likely related to the increased error in the PMF, as discussed above.

To summarize, we observed differences in the conformations of the water defects in the presence or absence of peptides for DOPE and DOPG. However, the hydration of the restrained lipid was not affected, as the number of hydrogen bonds with water was the same with and without peptide.

Lipid Desorption. The free energy difference between the lipid at equilibrium in the bilayer and in bulk water is the free energy for desorption ($\Delta G_{desorption}$). In contrast to ΔG_{flop}, there is a large effect of the peptides on $\Delta G_{desorption}$ (Table 2), except for DOPC. For DOPE, $\Delta G_{desorption}$ decreases by 37 and 27 kJ mol^{-1} with WALP23 and KALP23. DOPG showed a decrease in $\Delta G_{desorption}$ of 17 and 6 kJ mol^{-1} with WALP23 and KALP23 present. There are large errors for some of our free energies of desorption, likely due to poor sampling when the lipid is mostly in water but still interacting with the bilayer. The large difference in $\Delta G_{desorption}$ we observe for DOPG and DOPE with and without peptide is greater than the error we observe, except for DOPG with KALP23.

The restrained lipids stop interacting with the membrane at shorter distances from the bilayer center when a peptide is present. The order parameter S_z, averaged over the entire acyl chain, can be used to quantify this phenomenon, as in bulk water the lipids fold up, and its acyl chains are extended when interacting with the bilayer. S_z is calculated as follows:

$$S_z = \frac{1}{2}\langle 3\cos^2\theta_z - 1\rangle \quad (1)$$

θ_z is the molecular z axis of a carbon i of an acyl chain, corresponding to the axis formed by the carbons $i-1$ and $i+1$. The angled brackets in eq 1 mean that S_z is averaged over the two acyl chains of the two restrained lipids and over the simulation time. S_z varies between 1 and −0.5: 1 indicates a full alignment with the transmembrane axis (here, the z axis), 0.5 indicates a full alignment with the bilayer plane, and 0 indicates a random orientation. We note that an S_z of 0 could also mean a fixed angle of ca. 54.7°, but from the trajectory in our case the value of 0 is associated with a random orientation. In the absence of peptide, S_z increases from the bilayer center to a maximum of 0.45 when the lipid is partially removed from the membrane (Figure 4), meaning that the acyl chains are well aligned with the transmembrane axis. When the lipid is moved farther into bulk water, S_z suddenly drops to 0. This break point corresponds to the position at which the lipid folds onto itself and no longer interacts with the membrane. In the case of DOPG and DOPE, the maximum is lower when a peptide is present, and they become detached from the membrane 0.4−1.0 nm before DOPC (Figure 4). The decrease of S_z is not as drastic, fluctuating between 0 and 0.4 before stabilizing at 0, because DOPE and DOPG occasionally reestablish contacts with the bilayer before being fully desorbed. The large variation in S_z between ca. 2.5 and 4 nm indicates poor sampling in this region and explains the large error bars observed for $\Delta G_{desorption}$ (Table 2). Noteworthy, the peptides only weakly affect DOPC desorption (Figure 4).

DISCUSSION

Mechanism of Peptide-Mediated Lipid Flip-Flop. For all of our systems, as we moved the lipid headgroups toward the bilayer center, the free energy increases, and water is pulled into the bilayer to keep the headgroup solvated. It is energetically more favorable for the bilayer to deform and allow a water defect than for the lipid headgroup to become desolvated. No water pores were observed, consistent with our previous work on DOPC (*19*), although some other structures were observed: double and broken defects. A double defect corresponds to a water defect appearing on both sides of the bilayer. PC headgroups do not continuously line the water column, and there is no

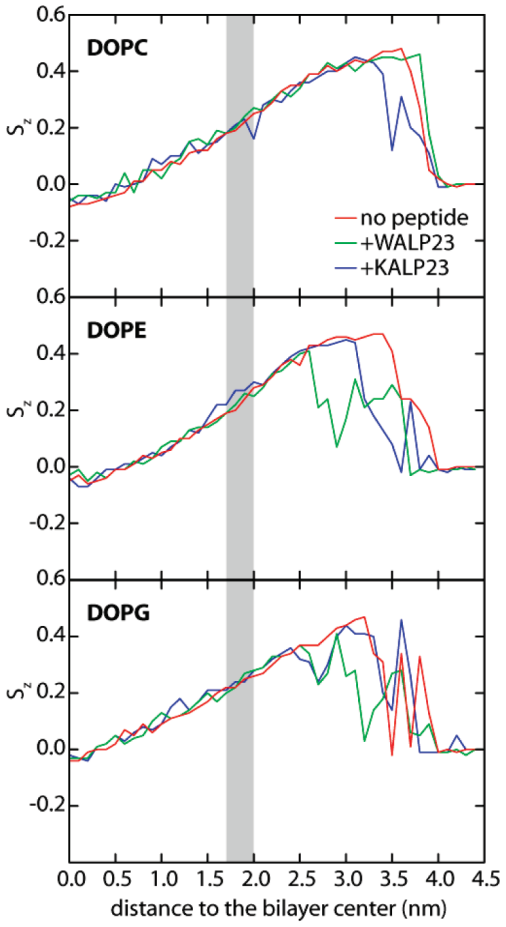

FIGURE 4: Order parameter S_z of the restrained lipid acyl chains as a function of the distance to the center of the bilayer. S_z is average over the trajectory and the whole acyl chain. The color code is the same for all panels.

transfer of water molecules through the membrane. A broken defect occurs when the water solvating the lipid at the center of the bilayer becomes disconnected from the bulk water. Consequently, the deformation of the membrane disappears, and the bilayer surface becomes almost flat. Double defects are more abundant in systems with DOPG, while broken defects appear more often in systems with DOPE. We speculate that DOPG's charged headgroup is able to pull water from the opposite leaflet, causing a double defect. The smaller headgroup of DOPE compared to DOPC might allow broken defects to form, as a larger headgroup would deform the structure of the bilayer more, allowing water to enter more easily. The existence of broken and double defects increases the difficulty of sampling the energy when the restrained lipid is close to the bilayer center. The error estimate of the PMFs becomes larger when lipids are restrained closer to the center of the bilayer (Figure 1).

We observed broken and double defects more frequently when a peptide was present in the bilayer. In the case of DOPE and DOPG, the phosphate density maps (Figure 2) show that the membrane surface is less perturbed and the phosphates penetrate less deeply into the hydrophobic core of the bilayer. The restrained lipid, and therefore water defect, always remained close to the peptide, suggesting preferential interactions of the pulled lipid and the peptide (Table 2). Remarkably, this interaction does not seem to have a large effect on the free energy barrier for flip-flop. We note that the lipid hydration was not affected by WALP23 or KALP23 (Figure 3). Taken together, these results suggest transmembrane peptides affect the formation and structure of the water defect during lipid flip-flop with a relatively modest effect on the free energy barrier. The increased frequency of double and broken defects with the presence of peptide might help to explain the mechanism of peptide induced flip-flop.

First, broken defects suggest the peptide's presence can substitute for the existence of a large, stable water defect. We have shown previously that there is a strong correlation between defect formation and PMF slope (*18*, *19*). In cells, large bilayer deformations, besides being energetically unfavorable, might be physiologically deleterious. In general, bilayers function as semipermeable membranes. We have shown previously that in pure bilayers DLPC, DMPC, POPC, and DPPC flip-flop occurs through a pore-mediated mechanism (*19*). As well, it has been shown that PC lipids can rapidly diffuse across preformed pores (*16*). Integral membrane proteins may allow flip-flop without large defect and pore formation.

Second, the increased observation of double defects may provide a transition state for flip-flop. For DOPC in a pure DOPC bilayer, we observe a single-sided water defect that is stable for the length of the simulation. For flip-flop, the defect would presumably form on the opposite leaflet and dissipate on the original leaflet. It is unclear whether a transient pore would form, the time scale of the transition, and if another free energy barrier exists. The observation of double defects in the simulations alleviates the ambiguity, as they provide a transition state for translocation. We suggest the presence of peptides could allow lipids to undergo flip-flop in a pore-independent mechanism.

The insertion of a positively charged arginine side chain analogue into a POPC bilayer containing between 15% and 55% mass fraction of hydrophobic or partially polar helices was investigated using MD simulations (*33*). It was shown that increasing the protein content in the bilayer decreased the energy barrier for arginine insertion, especially for the polar helices. The helices were shown to stabilize the formation of water defects in the membrane, in contrast to our results. This could be due to the increased number of helices used in ref *33*, with 6 helices in a 128 lipid bilayer being the lowest concentration (15% mass fraction), compared to our 1 helix and 64 lipids. The reduction in the energy barrier for arginine insertion was much less pronounced for the hydrophobic peptides compared to the polar peptides. Increasing the number of helices in our simulations, and investigating the effect of polar residues in the peptide, might reduce the energy barrier for flip-flop. As various cellular membranes can contain between 18% (myelin membranes of neurons) and 76% (inner mitochorial membrane) protein (*34*), and membrane proteins can have lipid-exposed polar side chains, this would be a biologically relevant system.

Rates of Flip-Flop and Comparison with Experiment. In a pure DOPC bilayer, the free energy barriers for DOPC, DOPE, and DOPG flip-flop calculated from our PMFs were 87, 103, and 105 kJ mol^{-1}. Experimental values for analogues of PC, PE, and PG are 113, 109, and 105 kJ mol^{-1}, in palmitoyloleoyl-PC (POPC) vesicles (*35*), although there is considerable spread in experimental values for the same type of lipid depending on the type of experiment and conditions. Experiments have been carried out with pyrene-labeled lipids, while unmodified lipids were used here, which might explain part of the discrepancy, although it is not clear why this would specifically affect DOPC.

With a WALP23 or a KALP23 peptide in the bilayer, ΔG_{flop} for DOPC remained unchanged, while it decreased by a few

kJ mol^{-1} for DOPE and DOPG. It is possible to evaluate ΔG_{flop} from experimental measurements of the flip-flop rate. Assuming the transition state for flip-flop is when the lipid is at the center of the bilayer, the following formula can be applied (*15*):

$$\Delta G_{flop} = -RT \ln \frac{k_f}{k_d} \quad (2)$$

Here, k_f is the rate of water defect formation, k_d the rate of water defect dissipation, R the gas constant, and T the temperature. k_f can be equated to the experimental flop rate if we assume that the lipid reaching the bilayer center is the rate-limiting step for flip-flop. k_d is assumed to be the same in the different systems. According to eq 2, an increase of k_f by 1 order of magnitude would correspond to a decrease of ΔG_{flop} by 5.7 kJ mol^{-1} (2.2kT). This is in the same range as the error estimate for some of our PMF calculations, such as DOPG. Experimental results showed that the flip-flop rate of a DOPE analogue increased by approximately 1 order of magnitude in the presence of WALP23 or KALP23 in vesicles reconstituted from *Escherichia coli* total lipid extract (1:250 peptide:lipid molar ratio (*13*)). From eq 2, the decrease in the free energy barrier would be around 6 kJ mol^{-1}. For a DOPG analogue, the decrease would be roughly 6 and 12 kJ mol^{-1} in the presence of WALP23 and KALP23, respectively (*13*, *14*). Experiments in pure DOPC vesicles have shown a similar trend, although no difference between WALP23 and KALP23 for DOPG was observed (*12*). Those experiments also showed that the flip-flop of a DOPC analogue was not affected by the presence of peptides (*14*), as observed in our simulations.

Comparison with experiment is limited by the lack of an accurate measure of the flop rate in the absence of peptides (*12*, *13*). A recent study employing time-resolved small angle neutron scattering, using unlabeled POPC and POPA, showed that neither POPC nor POPA flip-flop was enhanced in the presence of KALP23 peptides (*36*). This result is in direct qualitative disagreement with the above-mentioned studies of Kol et al. The use of different membrane environments and experimental conditions discourages direct comparison. For example, the use of lipid analogues compared to natural lipids could affect the observed differences. Many early experiments demonstrating the effect of transmembrane peptides and proteins on lipid flip-flop have been carried out with lipid analogues with their *sn*-2 chain replaced by a fluorescent compound (e.g., nitrobenzoxadiazole, NBD) attached to a short C6 acyl chain. Such voluminous and hydrophilic compounds affect the translocation of lipids (*37*−*39*) and might affect the rate of lipid flip-flop in the presence of transmembrane peptides. Stopped-flow assays have shown that the transmembrane diffusion of NBD-labeled PE and PC lipids was up to 1 order of magnitude slower than that of spin-labeled lipids (*38*). Furthermore, recent sum-frequency vibrational spectroscopy (SFVS) experiments have shown that the flip-flop rate of DPPC was 2 orders of magnitude higher than its spin-labeled counterpart (*39*). Our results cannot resolve this discrepancy due to the large errors we observe in our PMFs for lipid flip-flop, as well as methodological differences. In the future, similar calculations on lipid analogues might be informative as well as a more systematic look at lipid headgroups and tails. Investigating the effect of other integral membrane peptides and proteins will also be possible in the future.

Effect of the Peptides on the Desorption Free Energy. Our desorption free energies for DOPC and DOPE are in good agreement with experimental data (83 and 89 kJ mol^{-1} vs 92 and 95 kJ mol^{-1}, respectively (*35*)) but not for DOPG (62 kJ mol^{-1} vs 94 kJ mol^{-1} (*35*)). Notably, experimental free energies are for pyrene-labeled lipids desorbed from POPC vesicles, while natural lipids and pure DOPC bilayers were used here. There are substantial statistical errors in many of our free energies for desorption, so we will focus on the large effect of the presence of peptide that we observe.

The effect of the presence of a peptide on lipid chemical potential is important for general protein and lipid trafficking. How membrane proteins and lipids are sorted between membrane organelles remains debated. Membrane protein and lipid sorting is thought to be determined by hydrophobic mismatch; proteins with thick hydrophobic transmembrane segments would partition to membranes of a similar thickness (*40*). The lateral organization of the different cellular membranes has been suggested to influence protein and lipid trafficking (*41*). As well, the shape of lipids, such as the nonlamellar-forming lipids PE and PG, has been used to explain lipid sorting between membranes with different curvature (*42*). These three explanations are not mutually exclusive. From thermodynamics, the chemical potential of each lipid and protein molecule in different membrane environments determines membrane sorting. The complexity of lipid mixing makes this problem intractable and explains the use of conceptual models. We have determined the excess chemical potential of a DOPC, DOPE, and DOPG lipid in a DOPC bilayer, with and without model peptides.

It has been shown that many peptides induce nonlamellar structures in model bilayers (*43*−*46*). Of relevance, WALP and KALP peptides of various lengths were shown to increase nonlamellar structures, especially for PE and PG lipids (*47*). Our calculations provide atomistic resolution thermodynamic insight into the interaction between model peptides and phospholipids with different headgroups. In the bilayer containing WALP23 and KALP23, the excess chemical potential of DOPE and DOPG decreased, in contrast to DOPC, which was not significantly affected. The decreased chemical potential of DOPG and DOPE in the presence of peptide suggests these lipids prefer bilayers without peptide, or alternatively KALP23 and WALP23 destabilize nonlamellar-forming lipids. Both with and without peptide, the DOPC bilayer is lamellar in our simulations. Therefore, bilayer curvature and lipid shape cannot explain the drop in excess chemical potential that we observe. Recent computational studies (*48*) and experiments (*49*) suggest that membrane curvature and lipid shape are not a dominant force in lipid sorting. Calculations similar to ours, but on curved bilayers, would be an interesting test for the effect of bilayer curvature. Investigations using different lengths of WALP and KALP peptides, and lipid tails, might explain the effect of hydrophobic mismatch.

CONCLUSION

We have calculated free energy profiles for the transfer of single DOPC, DOPE, and DOPG molecules from bulk water to the center of a DOPC lipid bilayer, in the presence and absence of WALP23 or KALP23 transmembrane peptides. With a transmembrane peptide, the free energy barrier for DOPE and DOPG flip-flop decreased by a few kilojoules per mole, although this is close to the statistical error. In contrast, the free energy barrier for DOPC flip-flop was not affected by WALP or KALP. Consistent with previous work, the transmembrane diffusion of phospholipid headgroups into the bilayer interior created a water defect. For DOPE and DOPG in the presence of peptides, water defects

were smaller and less perturbing compared to DOPC. Broken and double water defects in the membrane occurred for DOPE and DOPG, particularly in the presence of peptide. These results suggest that transmembrane peptides facilitate PE and PG flip-flop by limiting deformations of the membrane and/or stabilizing transient configurations. We observed a large decrease in the free energy of desorption, or the excess chemical potential, for DOPE and DOPG in the presence of peptides (6−37 kJ mol^{-1}) but not for DOPC. The presence of WALP23 and KALP23 destabilizes DOPE and DOPG lipids, making it easier for them to become desorbed. Future studies are needed to understand the driving forces responsible for this behavior.

REFERENCES

1. Daleke, D. L. (2008) Regulation of phospholipid asymmetry in the erythrocyte membrane. *Curr. Opin. Hematol. 15*, 191–195.
2. van Meer, G., Voelker, D. R., and Feigenson, G. W. (2008) Membrane lipids: where they are and how they behave. *Nat. Rev. Mol. Cell Biol. 9*, 112–124.
3. Bevers, E. M., Comfurius, P., van Rijn, J. L., Hemker, H. C., and Zwaal, R. F. (1982) Generation of prothrombin-converting activity and the exposure of phosphatidylserine at the outer surface of platelets. *Eur. J. Biochem. 122*, 429–436.
4. Bevers, E. M., Comfurius, P., and Zwaal, R. F. (1983) Changes in membrane phospholipid distribution during platelet activation. *Biochim. Biophys. Acta 736*, 57–66.
5. Fadok, V. A., Voelker, D. R., Campbell, P. A., Cohen, J. J., Bratton, D. L., and Henson, P. M. (1992) Exposure of phosphatidylserine on the surface of apoptotic lymphocytes triggers specific recognition and removal by macrophages. *J. Immunol. 148*, 2207–2216.
6. Herrmann, A., Zachowski, A., and Devaux, P. F. (1990) Protein-mediated phospholipid translocation in the endoplasmic reticulum with a low lipid specificity. *Biochemistry 29*, 2023–2027.
7. Buton, X., Morrot, G., Fellmann, P., and Seigneuret, M. (1996) Ultrafast glycerophospholipid-selective transbilayer motion mediated by a protein in the endoplasmic reticulum membrane. *J. Biol. Chem. 271*, 6651–6657.
8. Kol, M. A., de Kruijff, B., and de Kroon, A. I. (2002) Phospholipid flip-flop in biogenic membranes: what is needed to connect opposite sides. *Semin. Cell Dev. Biol. 13*, 163–170.
9. Kornberg, R. D., and McConnell, H. M. (1971) Inside-outside transitions of phospholipids in vesicle membranes. *Biochemistry 10*, 1111–11120.
10. Rothman, J. E., and Kennedy, E. P. (1977) Rapid transmembrane movement of newly synthesized phospholipids during membrane assembly. *Proc. Natl. Acad. Sci. U.S.A. 74*, 1821–1825.
11. Huijbregts, R. P., de Kroon, A. I., and de Kruijff, B. (1998) Rapid transmembrane movement of newly synthesized phosphatidylethanolamine across the inner membrane of *Escherichia coli*. *J. Biol. Chem. 273*, 18936–18942.
12. Kol, M. A., van Laak, A. N., Rijkers, D. T., Killian, J. A., de Kroon, A. I., and de Kruijff, B. (2003) Phospholipid flop induced by transmembrane peptides in model membranes is modulated by lipid composition. *Biochemistry 42*, 231–237.
13. Kol, M. A., de Kroon, A. I., Rijkers, D. T., Killian, J. A., and de Kruijff, B. (2001) Membrane-spanning peptides induce phospholipid flop: a model for phospholipid translocation across the inner membrane of *E. coli*. *Biochemistry 40*, 10500–10506.
14. Kol, M. A., van Dalen, A., de Kroon, A. I., and de Kruijff, B. (2003) Translocation of phospholipids is facilitated by a subset of membrane-spanning proteins of the bacterial cytoplasmic membrane. *J. Biol. Chem. 278*, 24586–24593.
15. Tieleman, D. P., and Marrink, S. J. (2006) Lipids out of equilibrium: energetics of desorption and pore mediated flip-flop. *J. Am. Chem. Soc. 128*, 12462–12467.
16. Gurtovenko, A. A., and Vattulainen, I. (2007) Molecular mechanism for lipid flip-flops. *J. Phys. Chem. B 111*, 13554–13559.
17. Gurtovenko, A. A., Onike, O. I., and Anwar, J. (2008) Chemically induced phospholipid translocation across biological membranes. *Langmuir 24*, 9656–9660.
18. Bennett, W. F., MacCallum, J. L., and Tieleman, D. P. (2009) Thermodynamic analysis of the effect of cholesterol on dipalmitoylphosphatidylcholine lipid membranes. *J. Am. Chem. Soc. 131*, 1972–1978.
19. Sapay, N., Bennett, W. F. D., and Tieleman, D. P. (2009) Thermodynamics of flip-flop and desorption for a systematic series of phosphatidylcholine lipids. *Soft Matter 5*, 3295–3302.
20. Marrink, S. J., de Vries, A. H., and Tieleman, D. P. (2009) Lipids on the move: simulations of membrane pores, domains, stalks and curves. *Biochim. Biophys. Acta 1788*, 149–168.
21. Jorgensen, W. L., Maxwell, D. S., and Tirado-Rives, J. (1996) Development and testing of the OPLS all-atom force field on conformational energetics and properties of organic liquids. *J. Am. Chem. Soc. 118*, 11225–11236.
22. Berendsen, H. J. C., Postma, J. P. M., van Gunsteren, W. F., and Hermans, J. (1981) Intermolecular Forces (Pullman, B., Ed.) pp 331−342, Reidel, Dordrecht, Holland.
23. Tieleman, D. P., MacCallum, J. L., Ash, W. L., Kandt, C., Xu, Z. T., and Monticelli, L. (2006) Membrane protein simulations with a united-atom lipid and all-atom protein model: lipid-protein interactions, side chain transfer free energies and model proteins. *J. Phys.-Cond. Matter 18*, S1221–S1234.
24. Van Der Spoel, D., Lindahl, E., Hess, B., Groenhof, G., Mark, A. E., and Berendsen, H. J. (2005) GROMACS: fast, flexible, and free. *J. Comput. Chem. 26*, 1701–1718.
25. Darden, T., York, D., and Pedersen, L. (1993) Particle mesh Ewald—an N.Log(N) method for Ewald sums in large systems. *J. Chem. Phys. 98*, 10089–10092.
26. Essmann, U., Perera, L., Berkowitz, M. L., Darden, T., Lee, H., and Pedersen, L. G. (1995) A smooth particle mesh Ewald method. *J. Chem. Phys. 103*, 8577–8593.
27. Berendsen, H. J. C., Postma, J. P. M., Vangunsteren, W. F., Dinola, A., and Haak, J. R. (1984) Molecular-dynamics with coupling to an external bath. *J. Chem. Phys. 81*, 3684–3690.
28. Hess, B., Bekker, H., Berendsen, H. J. C., and Fraaije, J. G. E. M. (1997) LINCS: a linear constraint solver for molecular simulations. *J. Comput. Chem. 18*, 1463–1472.
29. Miyamoto, S., and Kollman, P. A. (1992) Settle—an analytical version of the shake and rattle algorithm for rigid water models. *J. Comput. Chem. 13*, 952–962.
30. MacCallum, J. L., Bennett, W. F., and Tieleman, D. P. (2008) Distribution of amino acids in a lipid bilayer from computer simulations. *Biophys. J. 94*, 3393–3404.
31. Bouzida, D., Kumar, S., and Swendsen, R. H. (1992) Efficient Monte Carlo methods for the computer simulation of biological molecules. *Phys. Rev. A 45*, 8894–8901.
32. Humphrey, W., Dalke, A., and Schulten, K. (1996) VMD: visual molecular dynamics. *J. Mol. Graphics 14*, 33–38.
33. Johansson, A. C., and Lindahl, E. (2009) Protein contents in biological membranes can explain abnormal solvation of charged and polar residues. *Proc. Natl. Acad. Sci. U.S.A. 106*, 15684–15689.
34. Guidotti, G. (1972) Membrane proteins. *Annu. Rev. Biochem. 41*, 731–752.
35. Homan, R., and Pownall, H. J. (1988) Transbilayer diffusion of phospholipids: dependence on headgroup structure and acyl chain length. *Biochim. Biophys. Acta 938*, 155–166.
36. Nakano, M., Fukuda, M., Kudo, T., Matsuzaki, N., Azuma, T., Sekine, K., Endo, H., and Handat, T. (2009) Flip-flop of phospholipids in vesicles: kinetic analysis with time-resolved small-angle neutron scattering. *J. Phys. Chem. B 113*, 6745–6748.
37. Devaux, P. F., Fellmann, P., and Hervé, P. (2002) Investigation on lipid asymmetry using lipid probes: comparison between spin-labeled lipids and fluorescent lipids. *Chem. Phys. Lipids 116*, 115–134.
38. Marx, U., Lassmann, G., Holzhutter, H. G., Wustner, D., Muller, P., Hohlig, A., Kubelt, J., and Herrmann, A. (2000) Rapid flip-flop of phospholipids in endoplasmic reticulum membranes studied by a stopped-flow approach. *Biophys. J. 78*, 2628–2640.
39. Liu, J., and Conboy, J. C. (2005) 1,2-diacyl-phosphatidylcholine flip-flop measured directly by sum-frequency vibrational spectroscopy. *Biophys. J. 89*, 2522–2532.
40. Killian, J. A. (1998) Hydrophobic mismatch between proteins and lipids in membranes. *Biochim. Biophys. Acta 1376*, 401–415.
41. Simons, K., and Ikonen, E. (1997) Functional rafts in cell membranes. *Nature 387*, 569–572.
42. Gruner, S. M. (1985) Intrinsic curvature hypothesis for biomembrane lipid-composition—a role for nonbilayer lipids. *Proc. Natl. Acad. Sci. U.S.A. 82*, 3665–3669.
43. Epand, R. M. (1998) Lipid polymorphism and protein-lipid interactions. *Biochim. Biophys. Acta 1376*, 353–368.
44. Keller, S. L., Gruner, S. M., and Gawrisch, K. (1996) Small concentrations of alamethicin induce a cubic phase in bulk phosphatidylethanolamine mixtures. *Biochim. Biophys. Acta 1278*, 241–246.

45. Prenner, E. J., Lewis, R. N., Neuman, K. C., Gruner, S. M., Kondejewski, L. H., Hodges, R. S., and McElhaney, R. N. (1997) Nonlamellar phases induced by the interaction of gramicidin S with lipid bilayers. A possible relationship to membrane-disrupting activity. *Biochemistry 36*, 7906–7916.
46. Killian, J. A., de Jong, A. M., Bijvelt, J., Verkleij, A. J., and de Kruijff, B. (1990) Induction of non-bilayer lipid structures by functional signal peptides. *EMBO J. 9*, 815–819.
47. Strandberg, E., Morein, S., Rijkers, D. T. S., Liskamp, R. M. J., van der Wel, P. C. A., and Killian, J. A. (2002) Lipid dependence of membrane anchoring properties and snorkeling behavior of aromatic and charged residues in transmembrane peptides. *Biochemistry 41*, 7190–7198.
48. Cooke, I. R., and Deserno, M. (2006) Coupling between lipid shape and membrane curvature. *Biophys. J. 91*, 487–495.
49. Tian, A., and Baumgart, T. (2009) Sorting of lipids and proteins in membrane curvature gradients. *Biophys. J. 96*, 2676–2688.